

New Zinc Phosphates Decorated by Imidazole-Containing Ligands

Jian Fan,[†] Carla Slebodnick,[†] Ross Angel,[‡] and Brian E. Hanson^{*†}

Departments of Chemistry and Geosciences, Virginia Polytechnic Institute and State University, Blacksburg, Virginia 24061

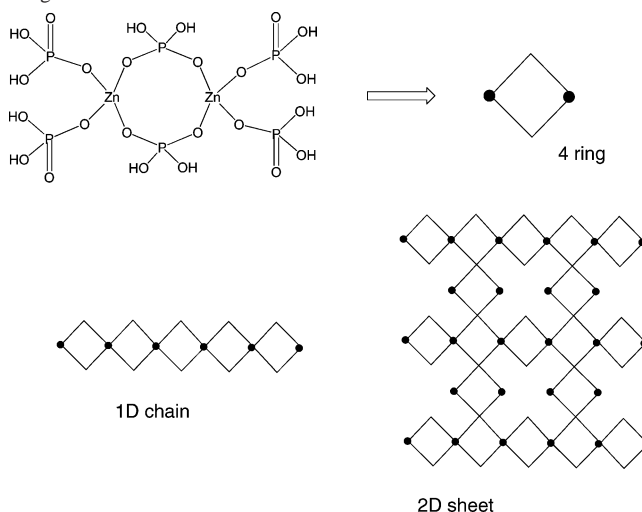
Received September 6, 2004

Four new zinc phosphates $[\text{Zn}(\text{HPO}_4)(\text{C}_6\text{H}_9\text{N}_3\text{O}_2)]$ (**1**), $[\text{Zn}(\text{HPO}_4)(\text{C}_4\text{H}_6\text{N}_2)]\cdot\text{H}_2\text{O}$ (**2**), $[\text{Zn}_2(\text{HPO}_4)_2(\text{C}_{14}\text{H}_{14}\text{N}_4)]\cdot 2\text{H}_2\text{O}$ (**3**), and $[\text{Zn}(\text{HPO}_4)(\text{C}_{14}\text{H}_{14}\text{N}_4)]$ (**4**) were synthesized in the presence of D-histidine, 1-methylimidazole, 1,4-bis-(imidazol-1-ylmethyl)benzene (L1), and 1,2-bis(imidazol-1-ylmethyl)benzene (L2), respectively, and their structures were determined by X-ray crystallography. The inorganic framework of compounds **1**, **2**, and **3** is composed of vertex-shared ZnO_3N and HPO_4 tetrahedra that form four rings, which, in turn, are linked to generate a one-dimensional ladder structure. In **1** and **2** the organic groups (monoimidazole ligand) are located at each side of the ladders, while in **3** the bisimidazole ligand, 1,4-bis(imidazol-1-ylmethyl)benzene, links the ladders together to form a novel 2D structure. Compound **1** is the first zinc phosphate framework to be templated by an N-bonded chiral amino acid. In **4** the zero-dimensional four rings are joined together by the linear bridging ligand, 1,2-bis(imidazol-1-ylmethyl)benzene, to generate a one-dimensional framework with a new face-to-face structural motif. The 3D structure of compound **4** is stabilized by hydrogen-bonding, π - π interactions, and $\text{C}-\text{H}\cdots\pi$ interactions. The approach of incorporating multifunctional ligands into zinc phosphate frameworks and linking the inorganic zinc phosphates subunits by an organic ligand provides opportunities for the design of new inorganic-organic open frameworks.

Introduction

Interest in zinc phosphate materials stems from their potential application in the areas of coatings, membranes, absorbents, and catalysis.¹ As a result, in recent years templated and ligand-modified zinc phosphates have been shown to have a rich structural chemistry.^{1–7} One common feature in the observed structures is the four ring, which may be isolated as a monomer, as, for example, in $[\text{N}(\text{CH}_3)_4\text{Zn}(\text{H}_2\text{PO}_4)_3]$ (Scheme 1),² $[\text{Zn}(2,2'\text{-bipy})_2(\text{H}_2\text{PO}_4)_4]$,³ and $[\text{C}_6\text{N}_2\text{H}_{18}][\text{Zn}(\text{H}_2\text{PO}_4)_2(\text{HPO}_4)]$.⁴ Furthermore, the monomers

Scheme 1. Schematic Drawings of Monomer and Condensed Four Rings Are Shown^a



^a The black dots represent zinc atoms.

may condense to form a variety of one- and two-dimensional structures and in some cases three-dimensional frameworks.^{2b,4,5} Some of the observed condensation pathways are indicated in Scheme 1. There is remarkable variety in the manner in

* To whom correspondence should be addressed. E-mail: hanson@vt.edu.

[†] Department of Chemistry.

[‡] Department of Geosciences.

- (1) (a) Gier, T. E.; Stucky, G. D. *Nature* **1991**, *349*, 508. (b) Cheetham, A. K.; Férey, G.; Loiseau, T. *Angew. Chem., Int. Ed.* **1999**, *38*, 3268. (c) Rao, C. N. R.; Natarajan, S.; Choudhury, A.; Neeraj, S.; Ayi, A. *Acc. Chem. Res.* **2001**, *34*, 80. (d) Harrison, W. T. A. *Curr. Opin. Solid State Mater. Sci.* **2002**, *6*, 407. (e) Yang, G.-Y.; Sevov, S. C. *J. Am. Chem. Soc.* **1999**, *121*, 8389. (f) Johnstone, J. A.; Harrison, W. T. A. *Inorg. Chem.* **2004**, *43*, 4567.
- (2) (a) Harrison, W. T. A.; Hanooman, L. *J. Solid State Chem.* **1997**, *131*, 363. (b) Dan, M.; Udayakumar, D.; Rao, C. N. R. *Chem. Commun.* **2003**, 2212.
- (3) Lin, Z.-E.; Zhang, J.; Zheng, S.-T.; Yang, G.-Y. *Inorg. Chem. Chem.* **2003**, *6*, 1035.
- (4) (a) Rao, C. N. R.; Natarajan, S.; Neeraj, S. *J. Am. Chem. Soc.* **2000**, *122*, 2810. (b) Neeraj, S.; Natarajan, S.; Rao, C. N. R. *J. Solid. State Chem.* **2000**, *150*, 417.

which the four rings may be ligated and linked. Yet, although many of the structures can be readily rationalized as deriving from the four rings, there are no rational syntheses available for a given structural motif. Indeed, the same templating or ligating group can lead to several different structures depending on temperature, concentration, and pH.⁶ However, it is recognized that the construction of extended structures via molecular building blocks offers great potential for the design of materials.⁷ For example, very recently the Natarajan group combined the principles of supramolecular organic chemistry with inorganic building units to form new zinc phosphate solids.^{5c}

The goal of our research is to synthesize zinc phosphates decorated by ancillary ligands and at the same time try to understand the role of the ancillary ligands in the formation of these solids. According to this approach, D-histidine, 1-methylimidazole, 1,4-bis(imidazol-1-ylmethyl)benzene, and 1,2-bis(imidazol-1-ylmethyl)benzene were used as ancillary ligands. Here, we report the synthesis, structure, and characterization of four new zinc phosphates: $[\text{Zn}(\text{HPO}_4)(\text{C}_6\text{H}_9\text{N}_3\text{O}_2)]$ (**1**), $[\text{Zn}(\text{HPO}_4)(\text{C}_4\text{H}_6\text{N}_2)]\cdot\text{H}_2\text{O}$ (**2**), $[\text{Zn}_2(\text{HPO}_4)_2(\text{C}_{14}\text{H}_{14}\text{N}_4)]\cdot 2\text{H}_2\text{O}$ (**3**), and $[\text{Zn}(\text{HPO}_4)(\text{C}_{14}\text{H}_{14}\text{N}_4)]\cdot\text{H}_2\text{O}$ (**4**). Compounds **1** and **2** have the same framework backbone, an edge-shared ladder structure. In **3** edge-shared ladder structures, as observed in **1** and **2**, are linked by 1,4-bis(imidazol-1-ylmethyl)benzene to form a novel 2D structure. In **4** the linear ligand 1,2-bis(imidazol-1-ylmethyl)benzene connects the four-ring building blocks to generate a new structural motif with the four rings linked face-to-face.

Experimental Section

Materials and Measurements. All commercially available chemicals are of reagent grade and used as received without further purification. The ligands 1,4-bis(imidazol-1-ylmethyl)benzene^{8a,b} and 1,2-bis(imidazol-1-ylmethyl)benzene^{8c} were synthesized by the reaction of imidazole with α,α' -dibromo-*p*-xylene and α,α' -dibromo-*o*-xylene, respectively, with the same procedures reported for preparation of 1,3,5-tris(imidazol-1-ylmethyl)-2,4,6-trimethylbenzene.⁹ Elemental analyses of C, H, and N were performed by Galbraith Laboratories, Inc. Thermogravimetric measurements were performed on a TA Instruments Q500 thermal analyzer in N_2 with the heating rate of $10\text{ }^\circ\text{C min}^{-1}$.

$[\text{Zn}(\text{HPO}_4)(\text{C}_6\text{H}_9\text{N}_3\text{O}_2)]$ (**1**). Hydrothermal treatment of zinc oxide (81.4 mg, 1.0 mmol), phosphoric acid (85 wt %, 230.6 mg,

2.0 mmol), sodium hydroxide (80.0, 2.0 mmol), D-histidine hydrochloride (383.2 mg, 2.0 mmol), and water (6 mL) for 10 days at $125\text{ }^\circ\text{C}$ yields a colorless needle crystalline product. Yield: 82% on the basis of zinc source. FT-IR (cm^{-1}): 3133(w), 3002(w), 2926(w), 1618(m), 1586(m), 1492(m), 1414(m), 1344(m), 1310(m), 1310(m), 1270(m), 1101(s), 1082(s), 992(s), 971(s), 911(s), 847(s), 770(m), 752(m), 683(s), 664(s). Anal. Calcd for $\text{C}_6\text{H}_9\text{N}_3\text{O}_6\text{PZn}$: C, 22.77; H, 3.18; N, 13.28. Found: C, 22.52; H, 3.43; N, 13.09.

$[\text{Zn}(\text{HPO}_4)(\text{C}_4\text{H}_6\text{N}_2)]\cdot\text{H}_2\text{O}$ (**2**). Hydrothermal treatment of zinc nitrate hexahydrate (297.5 mg, 1.0 mmol), phosphoric acid (85 wt %, 230.6 mg, 2.0 mmol), 1-methylimidazole (492.7 mg, 6.0 mmol), and water (6 mL) for 10 days at $125\text{ }^\circ\text{C}$ yields a colorless microcrystalline product. This sample was allowed to stand in the mother liquid for several weeks, and then needle crystals were collected. Yield: 31% on the basis of zinc source. FT-IR (cm^{-1}): 3377(w), 3125(m), 2929(w), 1544(m), 1530(m), 1290(w), 1254(w), 1207(w), 1141(m), 1021(s), 955(m), 911(m), 861(m), 848(m), 780(m), 770(m), 675(m). Anal. Calcd for $\text{C}_4\text{H}_9\text{N}_2\text{O}_5\text{PZn}$: C, 18.37; H, 3.47; N, 10.71. Found: C, 18.16; H, 3.49; N, 10.58. The weight loss (26 to $\sim 159\text{ }^\circ\text{C}$) corresponds to the loss of lattice water molecules (obsd 7.0%, $1\text{H}_2\text{O}$ calcd 6.9%). This compound is stable up to $197\text{ }^\circ\text{C}$ as shown in the TGA curve.

$[\text{Zn}_2(\text{HPO}_4)_2(\text{C}_{14}\text{H}_{14}\text{N}_4)]\cdot 2\text{H}_2\text{O}$ (**3**). Hydrothermal treatment of zinc acetate dihydrate (65.8 mg, 0.3 mmol), potassium dihydrogenphosphate (81.6 mg, 0.6 mmol), 1,4-bis(imidazol-1-ylmethyl)benzene (71.4, 0.3 mmol), and water (6 mL) for 9 days at $130\text{ }^\circ\text{C}$ yields a needle crystalline product. Yield: 89% on the basis of zinc source. FT-IR (cm^{-1}): 3357(w), 3146(w), 3130(w), 1526(m), 1440(m), 1238(m), 1132(m), 1088(s), 1021(s), 952(m), 911(s), 844(m), 805(m), 735(s). Anal. Calcd for $\text{C}_{14}\text{H}_{20}\text{N}_4\text{O}_{10}\text{P}_2\text{Zn}_2$: C, 28.16; H, 3.38; N, 9.38. Found: C, 27.73; H, 3.56; N, 9.22. The weight loss (23 to $\sim 163\text{ }^\circ\text{C}$) corresponds to the loss of lattice water molecules (obsd 5.9%, $2\text{H}_2\text{O}$ calcd 6.0%). This compound is stable up to $312\text{ }^\circ\text{C}$ as shown in the TGA curve.

$[\text{Zn}(\text{HPO}_4)(\text{C}_{14}\text{H}_{14}\text{N}_4)]\cdot\text{H}_2\text{O}$ (**4**). Hydrothermal treatment of zinc acetate dihydrate (65.8 mg, 0.3 mmol), potassium dihydrogenphosphate (81.6 mg, 0.6 mmol), 1,2-bis(imidazol-1-ylmethyl)benzene (71.4, 0.3 mmol), and water (6 mL) for 5 days at $125\text{ }^\circ\text{C}$ yields a block crystalline product. Yield: 81% on the basis of zinc source. FT-IR (cm^{-1}): 3422(w), 3127(m), 1529(m), 1520(m), 1455(m), 1445(m), 1364(m), 1280(w), 1250(w), 1106(s), 1071(s), 1028(m), 979(m), 952(s), 890(m), 844(m), 764(s), 748(s). Anal. Calcd for $\text{C}_{14}\text{H}_{17}\text{N}_4\text{O}_5\text{PZn}$: C, 40.26; H, 4.10; N, 13.41. Found: C, 39.54; H, 4.37; N, 13.17. The weight loss (23 to $\sim 255\text{ }^\circ\text{C}$) corresponds to the loss of lattice water molecules (obsd 4.4%, $1\text{H}_2\text{O}$ calcd 4.3%). This compound is stable up to $311\text{ }^\circ\text{C}$ as shown in the TGA curve.

Crystallographic Analyses. Low-temperature (100 K) single-crystal X-ray diffraction measurements for complexes **1–4** were collected on a Oxford Diffraction Xcalibur2 diffractometer equipped with the Enhance X-ray source and a Sapphire 2 CCD detector. The data collection routine, unit cell refinement, and data processing were carried out with the program CrysAlis.¹⁰ The structure was solved by direct methods using SHELXS-97 and refined by full-matrix least-squares.¹¹ The final refinements involved an anisotropic model for all non-hydrogen atoms. Hydrogen atoms were either located from the residual e^- density map and refined independently or located by a riding model. The crystal parameters, data collection, and refinement results for compounds **1–4** are summarized in Table

- (5) (a) Liu, W.; Liu, Y.; Shi, Z.; Pang, W. *J. Mater. Chem.* **2000**, *10*, 1451. (b) Ayi, A. A.; Choudhury, A.; Natarajan, S.; Rao, C. N. R. *J. Mater. Chem.* **2001**, *11*, 1181. (c) Natarajan, S.; Wullen, L. V.; Klein, W.; Jansen, M. *Inorg. Chem.* **2003**, *42*, 6265. (d) Choudhury, A.; Neeraj, S.; Natarajan, S.; Rao, C. N. R. *J. Mater. Chem.* **2001**, *11*, 1537.
- (6) (a) Neeraj, S.; Natarajan, S. *Chem. Mater.* **2000**, *12*, 2753. (b) Choudhury, A.; Natarajan, S.; Rao, C. N. R. *Inorg. Chem.* **2000**, *39*, 4295.
- (7) (a) Férey, G. *J. Solid State Chem.* **2000**, *152*, 37. (b) Murugavel, R.; Walawalkar, D. M.; Roesky, H. W.; Rao, C. N. R. *Acc. Chem. Res.* **2004**, in press.
- (8) (a) Dahl, P. K.; Arnold, F. H. *Macromolecules* **1992**, *25*, 7051. (b) Abrahams, B. F.; Hoskins, B. F.; Robson, R.; Slizys, D. A. *Crysi-tEngComm* **2002**, *4*, 478. (c) Tan, H. Y.; Zhang, H. X.; Ou, H. D.; Kang, B. S. *Inorg. Chim. Acta* **2004**, *357*, 869.
- (9) (a) Sun, W. Y.; Fan, J.; Okamura, T.-a.; Xie, J.; Yu, K. B.; Ueyama, N. *Chem. Eur. J.* **2001**, *7*, 2557. (b) Liu, H. K.; Sun, W. Y.; Zhu, H. L.; Yu, K. B.; Tang, W. X. *Inorg. Chim. Acta* **1999**, *295*, 129.

(10) CrysAlis v1.171; Oxford Diffraction: Wroclaw, Poland, 2004.

(11) (a) Sheldrick, G. M. *SHELXS97, Program for Crystal Structure Determination*; University of Göttingen: Göttingen, Germany, 1997. (b) Sheldrick, G. M. *SHELXL97, Program for Crystal Structural Refinement*; University of Göttingen: Göttingen, Germany, 1997.

Table 1. Crystal Data and Structure Refinement Parameters for 1–4

structure parameter	1	2	3	4
empirical formula	C ₆ H ₁₀ N ₃ ·O ₃ PZn	C ₄ H ₆ N ₂ ·O ₃ PZn	C ₁₄ H ₂₀ N ₄ ·O ₁₀ P ₂ Zn ₂	C ₁₄ H ₁₇ N ₄ ·O ₃ PZn
fw	316.51	261.47	597.02	417.66
T/K	100	100	100	100
space group	<i>P</i> -1	<i>P</i> 2 ₁ / <i>n</i>	<i>P</i> -1	<i>P</i> -1
<i>a</i> /Å	5.191(2)	11.189(1)	9.419(1)	8.536(3)
<i>b</i> /Å	9.535(4)	5.226(1)	9.520(1)	9.914(3)
<i>c</i> /Å	10.775(3)	14.579(1)	13.247(1)	10.631(4)
α /deg	86.18(3)		76.692(9)	81.33(3)
β /deg	84.58(3)	95.930(7)	78.841(10)	74.62(3)
γ /deg	75.79(3)		66.443(10)	69.10(3)
<i>V</i> /Å ³	514.1(3)	847.9(1)	1052.71(19)	808.7(5)
<i>Z</i>	2	4	2	2
<i>D</i> _{calc} /g cm ⁻³	2.044	2.048	1.883	1.715
μ /mm ⁻¹	2.567	3.077	2.492	1.653
R1 ^a [<i>I</i> > 2 σ (<i>I</i>)]	0.0529	0.0238	0.0392	0.0340
wR2 ^b [<i>I</i> > 2 σ (<i>I</i>)]	0.1029	0.0269	0.0759	0.1032

^a R1 = $\sum||F_o| - |F_c||/\sum|F_o|$. ^b wR2 = $\{\sum[w(F_o^2 - F_c^2)^2]/\sum[w(F_o^2)^2]\}^{1/2}$, where $w = 1/[\sigma^2(F_o^2) + (aP)^2 + bP]$, $P = [(F_o^2) + 2(F_c^2)]/3$.

Table 2. Selected Bond Distances (Å) and Angles (deg) for 1–4^a

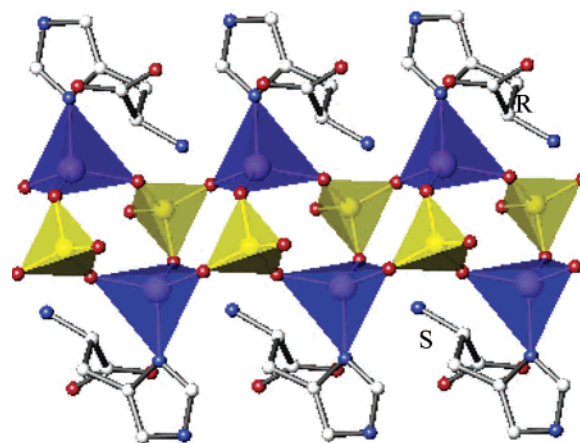
		1		
Zn1–O4 ^{#1}	1.926(4)	Zn1–N1	1.992(5)	
Zn1–O1 ^{#2}	1.915(4)	Zn1–O2	1.966(4)	
O1 ^{#2} –Zn1–O4 ^{#1}	116.16(18)	O1 ^{#2} –Zn1–O2	111.98(19)	
O4 ^{#1} –Zn1–O2	111.01(19)	O1 ^{#2} –Zn1–N1	108.5(2)	
O4 ^{#1} –Zn1–N1	103.2(2)	O2–Zn1–N1	105.0(2)	
		2		
Zn1–O2	1.929(1)	Zn1–O4 ^{#3}	1.936(1)	
Zn1–O1 ^{#4}	1.953(1)	Zn1–N2	1.998(2)	
O2–Zn1–O4 ^{#3}	115.34(5)	O2–Zn1–O1 ^{#4}	110.73(5)	
O4 ^{#3} –Zn1–O1 ^{#4}	107.46(5)	O2–Zn1–N2	104.08(6)	
O4 ^{#3} –Zn1–N2	112.32(6)	O1 ^{#4} –Zn1–N2	106.61(6)	
		3		
Zn1–O7	1.925(2)	Zn1–O2 ^{#5}	1.921(2)	
Zn1–O4	1.959(2)	Zn1–N42 ^{#6}	2.005(3)	
Zn2–O3	1.915(2)	Zn2–O5 ^{#7}	1.944(2)	
Zn2–O8	1.950(2)	Zn2–N12	1.993(3)	
O2 ^{#5} –Zn1–O7	109.74(9)	O2 ^{#5} –Zn1–O4	109.98(9)	
O7–Zn1–O4	110.60(9)	O2 ^{#5} –Zn1–N42 ^{#6}	105.31(9)	
O7–Zn1–N42 ^{#6}	120.47(9)	O4–Zn1–N42 ^{#6}	100.12(10)	
O3–Zn2–O5 ^{#7}	103.75(9)	O3–Zn2–O8	122.63(9)	
O5 ^{#7} –Zn2–O8	105.82(9)	O3–Zn2–N12	108.71(10)	
O5 ^{#7} –Zn2–N12	112.08(9)	O8–Zn2–N12	103.93(10)	
		4		
Zn1–O4	1.926(2)	Zn1–N12	1.983(2)	
Zn1–O2 ^{#8}	1.936(2)	Zn1–N22 ^{#9}	1.998(2)	
O4–Zn1–O2 ^{#8}	108.89(7)	O4–Zn1–N12	117.54(7)	
O2 ^{#8} –Zn1–N12	105.84(7)	O4–Zn1–N22 ^{#9}	98.72(8)	
O2 ^{#8} –Zn1–N22 ^{#9}	108.05(7)	N12–Zn1–N22 ^{#9}	117.37(8)	

^a Symmetry transformations used to generate equivalent atoms: #1, $-x, 1 - y, -z$; #2, $1 - x, 1 - y, -z$; #3, $1 - x, 1 - y, -z$; #4, $1 - x, -y, -z$; #5, $-x + 1, -y + 1, -z + 1$; #6, $x, y - 1, z - 1$; #7, $-x, -y + 2, -z + 1$; #8, $2 - x, 1 - y, z$; #9, $x, -1 + y, 1 + z$.

1. Selected bond length and angles are listed in Table 2. Further details are provided in the Supporting Information.

Results and Discussion

Description of the Crystal Structures. [Zn(HPO₄)(C₆H₉N₃O₂)] (1) and [Zn(HPO₄)(C₄H₆N₂)·H₂O] (2). The asymmetric unit of compound 1 contains one zinc atom, one phosphate, and one histidine as shown in Figure S1 (Supporting Information). Each zinc atom in compound 1 is coordinated by three oxygen atoms from three different phosphate groups and one nitrogen atom from histidine to

**Figure 1.** Ladder structure of compound 1 showing the connectivity of the PO₄ (yellow) and ZnO₃N (blue) tetrahedra to four-ring loops.

complete its tetrahedral coordination environment. A similar arrangement, plus an extra framework water molecule, is seen in compound 2 (see Figure S2 in the Supporting Information). Structural representations for 2 are given in the Supporting Information due to its close structural similarity to the histidine structure 1.) This kind of ZnO₃N binding set is characteristic of several nitrogen-donor-ligand-modified zinc phosphates.^{5b,6b,12} The tetrahedral coordination modes in compounds 1 and 2 have typical geometrical parameters.

Assuming the usual valences for Zn, P, and O as +2, +5, and –2, respectively, and a neutral zwitterionic histidine in 1, then the asymmetric unit has a net charge of –1. Accordingly, for charge balance a proton must reside on either the phosphate or carboxylate group. Because the pK_a of HPO₄^{2–} (12.3) is larger than that of the carboxylate group of histidine (1.8), it is the phosphate group that is protonated, making it monohydrogen phosphate. The identical situation occurs in 2; the additional proton can only be placed on a phosphate oxygen atom. To confirm these assignments the hydrogen was located in the residual e[–] density map and refined independently. Thus, each phosphorus atom makes three connections to neighboring zinc atoms through the bridging oxygen, and the terminal oxygen atom is formulated as a –OH group not an unsaturated =O atom. The longest P–O bond length in 1, 1.574(5) Å, corresponds to the terminal oxygen, consistent with this assignment. The ZnO₃N and HPO₄ groups are connected to form an edge-shared ladder structure composed of four rings that propagates along the [100] direction (Figure 1). The framework of compound 2 also consists of ladders composed of four rings onto which the 1-methylimidazole molecules are grafted (Figure S3, Supporting Information).

The histidine molecules in 1 and the methylimidazole ligands in 2 are attached to zinc atoms, extending to each side of the ladder structure. It is noteworthy that in 1 the histidine molecules on one side have the *R* absolute config-

- (12) (a) Harrison, W. T. A.; Phillips, M. L. F.; Stanchfield, J.; Neno, T. M. *Inorg. Chem.* **2001**, *40*, 895. (b) Drumel, S.; Janvier, P.; Deniaud, D.; Bujoli, B. *J. Chem. Soc., Chem. Commun.* **1995**, 1051. (c) Cui, A.; Yao, Y. *Chem. Lett.* **2001**, 1148. (d) Gordon, L. E.; Harrison, W. T. A. *Inorg. Chem.* **2004**, *43*, 1808. (e) Neeraj, S.; Natarajan, S.; Rao, C. N. R. *New J. Chem.* **1999**, 303.

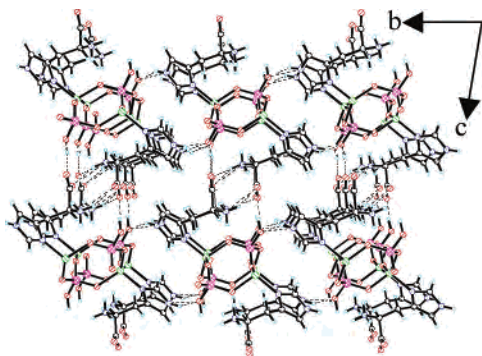


Figure 2. Crystal packing diagram for compound **1** in the *bc* plane. Dashed lines represent the various possible hydrogen-bond interactions. The eclipsed nature of the four rings is evident in this view, showing that the sheets are stacked in an AAA fashion.

uration and are related by an inversion center, as required by the *P*-1 space group, to the groups of *S* configuration on the other side of the ladder. As a result, this compound is achiral, though the starting histidine is homochiral (See Experimental Section). It is well known that histidine is racemized under both alkaline and acidic conditions at high temperature.¹³ Thus far, there are some reports of zinc phosphite or zinc phosphate templated by chiral organic groups,^{12d,14} but to the best of our knowledge, compound **1** is the first zinc phosphate phase to be templated by a chiral amino acid, although the resulting compound is obtained with racemic histidine.

Hydrogen bonding is an important factor in defining the molecular packing in zinc phosphates.^{12d} For example, Yu reported recently that racemic $[\text{Co}(\text{en})_3]^{3+}$ imparts chirality into the zinc phosphate framework via hydrogen bonding.¹⁵ As shown in Figure 2, the neutral [100] ladders in compound **1** are connected by means of hydrogen bonds, N2–H9...O3(1 + *x*, –1 + *y*, *z*), to form the pseudo-sheets along the [010] direction (Table 3). The sheets are further linked by hydrogen-bond interactions to form the 3D structure. The sheets configure themselves in an AAA arrangement along the [001] direction, and because the inversion center is contained within the core ladder motif, there are no chiral components to the structure. The packing diagram for **2** also shows the formation of sheets connected by hydrogen bonds in an AAA arrangement; however, the potential for hydrogen bonding in **2** is limited compared to the histidine structure, **1** (Figure S4, Supporting Information).

The ladder structures observed in **1** and **2** are stabilized by the imidazole-containing pendant ligands that bind zinc. To enhance our understanding of the various pathways for the formation of new solids, we wished to keep the basic four-ring unit intact while modifying the ligand to influence the assembly process. Thus, we tried to knit the ladder motif together into sheets by connecting them with bifunctional ligands, specifically bisimidazole ligands. We performed this reaction with the ligands 1,4-bis(imidazol-1-ylmethyl)ben-

Table 3. Distances (Å) and Angles (deg) of Hydrogen Bonding for **1–4**^a

D–H...A ^b	distance (D...A)	D–H–A	angle (D–H–A)
1			
N3–H6...O10 ^{#1}	2.901(7)	N3–H6–O10 ^{#1}	153
N3–H7...O10 ^{#2}	2.907(7)	N3–H7–O10 ^{#2}	172
N3–H8...O2 ^{#2}	2.859(7)	N3–H8–O2 ^{#2}	150
N2–H9...O3 ^{#3}	2.821(7)	N2–H9–O3 ^{#3}	153
O3–H10...O11 ^{#1}	2.528(6)	O3–H10–O11 ^{#1}	172
C2–H2...O11 ^{#4}	3.325(9)	C2–H2–O11 ^{#4}	133
C4–H4...O4 ^{#5}	3.275(8)	C4–H4–O4 ^{#5}	132
C5–H5...O2	3.276(8)	C5–H5–O2	169
2			
O5–H5A...O1 ^{#6}	2.810(2)	O5–H5A–O1 ^{#6}	172
O5–H5B...O3 ^{#7}	3.164(2)	O5–H5B–O3 ^{#7}	135
O5–H5B...O4 ^{#7}	2.836(2)	O5–H5B–O4 ^{#7}	158
O3–H6...O5 ^{#8}	2.614(2)	O3–H6–O5 ^{#8}	171
C1–H1...O5 ^{#9}	3.372(2)	C1–H1–O5 ^{#9}	159
C4–H4B...O4 ^{#10}	3.360(2)	C4–H4B–O4 ^{#10}	141
3			
O6–H1...O2W	2.590(4)	O6–H1–O2W	166
O1W–H1A...O4 ^{#11}	2.965(4)	O1W–H1A–O4 ^{#11}	174
O1W–H1B...O8 ^{#12}	2.781(3)	O1W–H1B–O8 ^{#12}	162
O1–H2...O1W	2.602(4)	O1–H2–O1W	173
O2W–H4A...O7 ^{#13}	2.833(4)	O2W–H4A–O7 ^{#13}	159
O2W–H4B...O4 ^{#14}	2.792(3)	O2W–H4B–O4 ^{#14}	165
C12–H12A...O1 ^{#14}	3.308(3)	C12–H12A–O1 ^{#14}	146
C41–H41B...O3 ^{#15}	3.282(4)	C41–H41B–O3 ^{#15}	134
4			
O5–HW1...O1 ^{#16}	2.892(3)	O5–HW1–O1 ^{#16}	156
O5–HW2...O2	2.818(3)	O5–HW2–O2	166
O3–H20...O1 ^{#16}	2.558(3)	O3–H20–O1 ^{#16}	178
C3–H3...O5 ^{#17}	3.318(3)	C3–H3–O5 ^{#17}	139
C12–H12...O2	3.327(3)	C12–H12–O2	147
C14–H14...O1 ^{#18}	3.289(3)	C14–H14–O1 ^{#18}	171
C21–H21B...O3 ^{#19}	3.249(3)	C21–H21B–O3 ^{#19}	160

^a Symmetry transformation used to generate equivalent atoms: #1, –*x*, 1 – *y*, 1 – *z*; #2, –1 + *x*, *y*, *z*; #3, 1 + *x*, –1 + *y*, *z*; #4, –*x*, –*y*, 1 – *z*; #5, –*x*, 1 – *y*, –*z*; #6, 1/2 + *x*, 1/2 – *y*, 1/2 + *z*; #7, 1 – *x*, –*y*, –*z*; #8, 1 – *x*, 1 – *y*, –*z*; #9, 3/2 – *x*, –1/2 + *y*, 1/2 – *z*; #10, 1/2 – *x*, –1/2 + *y*, 1/2 – *z*; #11, –*x*, 1 – *y*, 1 – *z*; #12, *x*, –1 + *y*, *z*; #13, 1 – *x*, 2 – *y*, 1 – *z*; #14, *x*, 1 + *y*, *z*; #15, –*x*, 2 – *y*, 2 – *z*; #16, 3 – *x*, 1 – *y*, –*z*; #17, 2 – *x*, 2 – *y*, –1 – *z*; #18, –1 + *x*, 1 + *y*, *z*; #19, 2 – *x*, 2 – *y*, –*z*. ^b D = donor; A = acceptor.

zene, L1, and 1,2-bis(imidazol-1-ylmethyl)benzene, L2, leading to the formation of compounds **3** and **4**, respectively. In **3** the observed structure forms sheets in the manner expected. However, in **4** a new linear structure was obtained in which the four-ring units are linked in a face-to-face fashion by L2.

[Zn₂(HPO₄)₂(C₁₄H₁₄N₄)·2H₂O (3) and [Zn(HPO₄)(C₁₄H₁₄N₄)·H₂O (4). The asymmetric unit of compound **3** contains two zinc atoms, two monohydrogen phosphate units, and one L1, which repeat to form the framework, and two extra framework water molecules (Figure S5, Supporting Information). The two independent zinc atoms are both tetrahedrally coordinated with the same O₃N binding set. For Zn1, (Zn–O)_{av} = 1.94 Å, O–Zn–O bond angles are in the range of 109.7–110.6° with an average value of 110.1°, and O–Zn–N bond angles are in the range 100.1–120.5° with an average of 108.6°. For Zn2, (Zn–O)_{av} = 1.93 Å, O–Zn–O bond angles are in the range of 103.8–122.6° with an average value of 110.7°, and O–Zn–N bond angles are in the range 103.9–112.1° with an average of 108.2°. Within each hydrogen phosphate unit three oxygen atoms bond to

(13) Greenstein, J. P.; Winitz, M. *Chemistry of the Amino Acids*; John Wiley & Sons: New York, 1961; Vol. 3, Chapter 27.

(14) Nenoff, T. M.; Thoma, S. G.; Provencio, P.; Maxwell, R. S. *Chem. Mater.* **1998**, *10*, 3077.

(15) Wang, Y.; Yu, J.; Shi, Z.; Xu, R. *Chem. Eur. J.* **2003**, *9*, 5048.

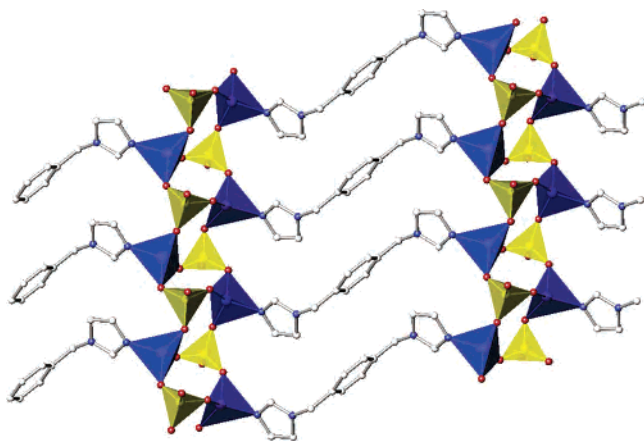


Figure 3. 2D structure of compound **3** showing the connectivity of PO₄ (yellow) and ZnO₃N (blue) tetrahedra to four-ring loops.

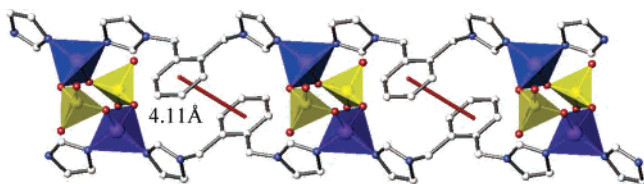


Figure 4. Polyhedral representation of the one-dimensional structure of compound **4** showing the connectivity of the PO₄ (yellow) and ZnO₂N₂ (blue) tetrahedra to four-ring loops. The face-to-face π - π interaction is indicated by the red line.

three zinc atoms and one -OH group is terminally bonded to phosphorus. The presence of a hydroxyl group is confirmed by the observation of a peak in the difference Fourier map corresponding to the hydrogen atom on the O1 and O6 atoms. The P–O distances are in the range of 1.51–1.58 Å for both hydrogen phosphate units.

In compound **3** the ZnO₃N and HPO₄ groups are connected to form an edge-shared ladder structure composed of four rings, as observed in **1** and **2** (Figure 3). Because there are two independent zinc atoms and two hydrogen phosphate groups within the one asymmetric unit as mentioned above, the four rings within one ladder structure are not identical and repeat in the *ABCDABCD* sequence as shown in Figure S6 (Supporting Information). In **3** the dihedral angles between the imidazole groups and the benzene ring are 77.6° and 77.2°, respectively, and the imidazole groups extend to each side of the benzene ring, in the opposite direction. Thus, the L1 ligand in **3** adopts the *trans*-conformation in a *Z*-type mode.^{8b}

In compounds **1** and **2** the ladder structures are linked by hydrogen bonds to generate the pseudo-sheet. These hydrogen bonds are derived from the interaction between the ancillary organic ligand within one ladder and the hydrogen phosphate group within the adjacent ladder (Figure 2 and Figure S4 (Supporting Information)). In **3** the inorganic ladders within a layer are parallel and linked together by L1 to form the 2D structure as desired. Two L1 units and four four rings form a macrocycle of 34 atoms. The layers of **3** are connected by hydrogen bonding to form the 3D structure in an *AAA* arrangement (Figure S7, Supporting Information). The solvated water molecules are located in the 3D structure

between layers by forming two O–H \cdots O(water) and four O(water)–H \cdots O hydrogen bonds.

Compounds **3** and **4** are synthesized under similar conditions; however, the structures are quite different due to the subtle difference between the ligands, L1 and L2. The asymmetric unit of compound **4** contains one zinc, one hydrogen phosphate, one bisimidazole benzene ligand, L2, and one extra framework water molecule (Figure S8, Supporting Information). Two nitrogen atoms from the two L2 units [$(\text{Zn}-\text{N})_{\text{av}} = 1.99 \text{ \AA}$] and two oxygen atoms from two phosphate groups [$(\text{Zn}-\text{O})_{\text{av}} = 1.93 \text{ \AA}$] tetrahedrally coordinate each zinc atom in **4**. The average bond angles for O–Zn–O, N–Zn–N, and O–Zn–N are 108.9°, 117.4°, and 107.5°, respectively. This kind of ZnO₂N₂ ligand set for zinc phosphates is rare.^{12c,16} Two hydrogen phosphate oxygen atoms bond to zinc to form bridges, and two oxygen atoms, a -OH group and an unsaturated =O atom, are terminally bonded to phosphorus. The P–O distances are in the range of 1.51–1.59 Å, which is similar to that in compounds **1–3**. The longest P–O distance of P1–O3 = 1.587(2) Å suggests that O3 is protonated. The presence of a hydroxyl group is confirmed by the observation of a peak in the difference Fourier map corresponding to the hydrogen atom on the O3 atom. Unlike the structures in **1–3**, the four rings in **4** are not fused to form a one-dimensional ladder structure. Instead, the four rings are bridged in one dimension by L2 ligands (see below).

In **4** the imidazole groups are essentially perpendicular to the benzene ring with dihedral angles of 85.9° and 90.5° for the two rings. In general, the pendant imidazol-1-ylmethyl groups of the L2 ligand adopt either a *trans*-conformation or a *cis*-conformation relative to the benzene ring.^{8c} It is interesting that in **4** both C(methylene group)–N(imidazole group) bonds are eclipsed, i.e., they extend nearly parallel to the benzene ring with torsion angles C2–C1–C11–N11 = 160.82(18)° and C1–C2–C21–N21 = –160.16(18)°. Thus, the L2 group can be regarded as a linear bridging ligand. This is a unique geometry for the L2 ligand. As illustrated in Figure 4 the strictly alternating ZnO₂N₂ and HPO₄ tetrahedral units give rise to the formation of four rings which are linked by the linear ligand to generate a new one-dimensional structure with the face-to-face structural motif. Thus, the Zn₂P₂ planes are parallel to each other, as required by symmetry, and separated by two L2 ligands. As mentioned above, within most zinc phosphate structures the four rings are connected by Zn–O–P linkages to generate higher dimensional frameworks. Recently, many zinc organophosphates have been synthesized in which the inorganic scaffold is connected by an organic group attached to the phosphorus atom.¹⁷ However, so far there are only a few examples of

(16) Ayi, A. A.; Neeraj, S.; Choudhury, A.; Natarajan, A.; Rao, C. N. R. *J. Phys. Chem. Solids*. **2001**, *62*, 1481.

(17) (a) Mao, J. G.; Wang, Z.; Clearfield, A. *New J. Chem.* **2002**, *26*, 1010. (b) Mao, J. G.; Clearfield, A. *Inorg. Chem.* **2002**, *41*, 2319. (c) Mao, J. G.; Wang, Z.; Clearfield, A. *Inorg. Chem.* **2002**, *41*, 2334. (d) Lei, C.; Mao, J. G.; Sun, Y. Q.; Zeng, H. Y.; Clearfield, A. *Inorg. Chem.* **2003**, *42*, 6157. (e) Zhang, B.; Poojary, D. M.; Clearfield, A. *Inorg. Chem.* **1998**, *37*, 1844. (f) Poojary, D. M.; Zhang, B.; Bellinghausen, P.; Clearfield, A. *Inorg. Chem.* **1996**, *35*, 5254.

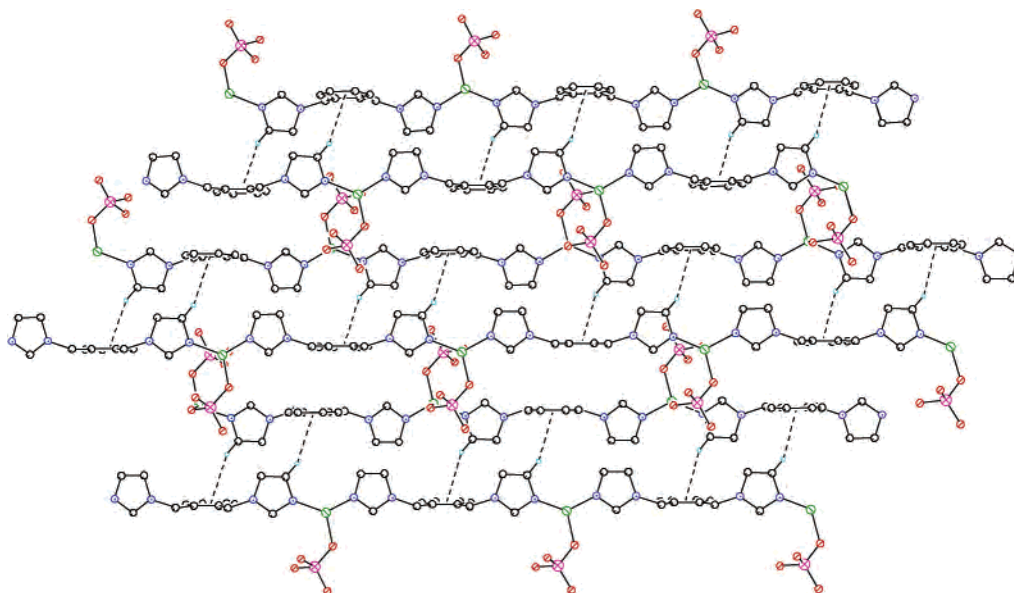
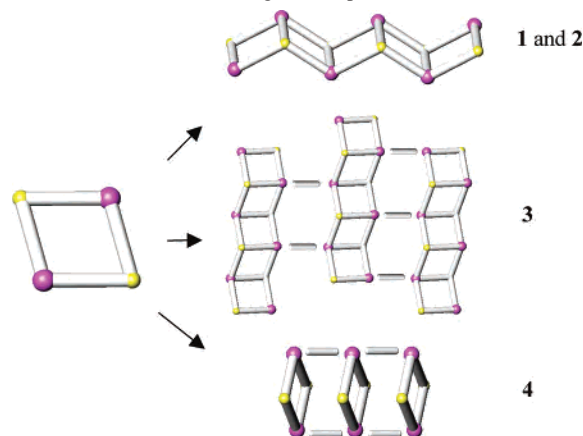


Figure 5. Pseudo-2D network of compound **4** with the C–H··· π interactions indicated by dashed lines.

Scheme 2. Schematic Drawing of Compounds **1–4**^a



^a The zinc phosphate four rings are depicted as parallelograms, and the bridging bisimidazole ligands are represented as bars.

zinc phosphate or zinc phosphite fragments directly connected by ligands bound to zinc.¹⁸

The two four rings that are connected by two L2 units in **4** form a macrocycle of 30 atoms. A centroid–centroid distance of 4.11 Å between two adjacent benzene rings within one macrocycle indicates the presence of face-to-face π – π interactions.¹⁹ Another striking feature of compound **4** is that C–H··· π interactions²⁰ associate the one-dimensional chains into a pseudo-2D structure as illustrated in Figure 5, which, in turn, is connected to form a 3D structure in an AAA arrangement by hydrogen-bonding interactions (Figure S9, Supporting Information). Such an interaction occurs between

the hydrogen atom (H13) bound to C13 (imidazole group) and the benzene ring of a neighboring chain. The C13–H13–X (X refers to the centroid of the benzene ring) angle is 155.7°, and the H···X distance is 2.98 Å. The solvated water molecules are located in the 3D structure by forming one C–H···O (water) and two O(water)–H···O hydrogen bonds with the neutral backbone.

Conclusion

Four new zinc phosphates have been synthesized in the presence of D-histidine, 1-methylimidazole, 1,4-bis(imidazol-1-ylmethyl)benzene, and 1,2-bis(imidazol-1-ylmethyl)benzene. Each structure is constructed from four-ring secondary building units that consist of two tetrahedral zinc atoms and two tetrahedral phosphate groups. In compounds **1** and **2** the monoimidazole ligands simply decorate the ladder structures that are formed from edge-fused four rings; however, in **3** the bisimidazole ligand L1 links the ladder structures together to form layers. In **4** the bisimidazole ligand L2 not only completes the zinc coordination sphere but also separates adjacent inorganic four rings to form chains (Scheme 2). The 3D structures of **1–3** are stabilized by hydrogen bonding, while in **4** three kinds of weak interactions, hydrogen bonding, π – π interactions, and C–H··· π interactions, are involved and play a subtle role in the formation of its 3D structure. The ability to design and control these interactions will enable supramolecular crystal engineering of metal phosphate materials. We are currently investigating additional bifunctional ligands in the construction of metal phosphate materials.

Acknowledgment. We thank R. J. Reynolds for support of this work through a McNair Postdoctoral Fellowship to J.F. We thank the NSF (grant CHE-0131128) for funding the purchase of the Oxford Diffraction Xcalibur2 single-crystal diffractometer. We thank Michael Vadala and Prof. J. Riffle for the TGA measurements.

- (18) (a) Halasyamani, P. S.; Drewitt, M. J.; O'Hare, D. *Chem. Commun.* **1997**, 867. (b) Lin, Z.; Zhang, J.; Zheng, S. T.; Yang, G. Y. *Microporous Mesoporous Mater.* **2004**, *68*, 65. (c) Rodgers, J. A.; Harrison, W. T. A. *Chem. Commun.* **2000**, 2385.
 (19) Hunter, C. A.; Sanders, J. K. M. *J. Am. Chem. Soc.* **1990**, *112*, 5525.
 (20) (a) Zhu, H. F.; Kong, L. Y.; Okamura, T.-a.; Fan, J.; Sun, W. Y.; Ueyama, N. *Eur. J. Inorg. Chem.* **2004**, 1465. (b) Caradoc-Davies, P. L.; Gregory, D. H.; Hanton, L. R.; Turnbull, J. M. *J. Chem. Soc., Dalton Trans.* **2002**, 1574. (c) Jitsukawa, K.; Iwai, K.; Masuda, H.; Ogoshi, H.; Einaga, H. *J. Chem. Soc., Dalton Trans.* **1997**, 3691.

Supporting Information Available: Figure S1, showing the asymmetric unit of **1**, Figure S2, showing the asymmetric unit of **1**, Figure S3, showing the ladder structure of **2**, Figure S4, showing the packing diagram of **2**, Figure S5, showing the asymmetric unit of **3**, Figure S6, zigzag arrangement of four rings in **3**, Figure S7,

showing the packing diagram of **3**, Figure S8, showing the ladder structure of **4**, Figure S9, showing the packing diagram of **4**, and X-ray crystallographic files in CIF format. This material is available free of charge via Internet at <http://pubs.acs.org>.

IC0487528